X–ray crystal structure, Hirshfeld surface analysis, DFT and electronic properties of (E)–4–chloro–N'–(2,4–dihydroxy–benzylidene) benzohydrazide

C. Arunagiri , A.G. Anitha , A. Subashini , N.K. Loknath

PII: S2405-8300(18)30206-4
DOI: https://doi.org/10.1016/j.cdc.2018.100174
Article Number: 100174
Reference: CDC 100174

To appear in: *Chemical Data Collections*

Received date: 24 September 2018
Revised date: 16 December 2018
Accepted date: 19 December 2018

Please cite this article as: C. Arunagiri , A.G. Anitha , A. Subashini , N.K. Loknath , X–ray crystal structure, Hirshfeld surface analysis, DFT and electronic properties of (E)–4–chloro–N'–(2,4–dihydroxy–benzylidene) benzohydrazide, *Chemical Data Collections* (2018), doi: https://doi.org/10.1016/j.cdc.2018.100174

X–ray crystal structure, Hirshfeld surface analysis, DFT and electronic properties of (*E*)–4–chloro–*N*'–(2,4–dihydroxy–benzylidene) benzohydrazide

C. Arunagiri [a]*, A. G. Anitha [b], A. Subashini [c], N. K. Loknath[d]

[a] PG & Research Department of Physics, Periyar E.V.R. College (Autonomous), Tiruchirappalli – 620 023, Tamil Nadu, India.

[b]PG & Research Department of Physics, Seethalakshmi Ramaswami College (Autonomous), Tiruchirappalli – 620 002, Tamil Nadu, India.

[c]PG & Research Department of Chemistry, Seethalakshmi Ramaswami College (Autonomous), Tiruchirappalli – 620 002, Tamil Nadu, India.

[d] Department of Physics, University of Mysore, Mysore – 570 006, India.

Abstract

A new compound of the title Schiff base ($C_{14}H_{11}ClN_2O_3$) was synthesized and characterized by using spectroscopic tools such as IR, NMR (^{1}H and ^{13}C), UV visible spectral and finally the structure was confirmed by the single crystal X–ray diffraction studies. The compound was crystallized in the monoclinic crystal system, with the space group $P2_1/c$. The unit cell parameters were confirmed by single crystal X–ray diffraction. The molecular packing is controlled by intermolecular hydrogen bonds and π–π stacking interactions. The crystal and molecular structure of the title Schiff base are linked via few intermolecular O–H···O, N–H···O hydrogen bond and an intramolecular O–H···N hydrogen bond. Geometrical parameters have been carried out by the computational density functional theory (DFT) B3LYP/6–311G (d,p) and compared with the XRD values. Further, Hirshfeld surface and electrostatic potential surface analysis were carried out to understand the intermolecular interactions along with their graphical visualization.

Keywords: Crystal structure; X–ray diffraction; π–π stacking interaction; Hirshfeld analysis; Density functional theory.

*Corresponding author's. Tel.: +91 8903178736.

E –mail address: arunasuba03@gmail.com (C. Arunagiri).

Specifications table

Subject area	*Organic Chemistry and X–ray Crystallography*
Compound	*(E)–4–chloro–N'–(2,4–dihydroxy–benzylidene)benzohydrazide.*
Data category	*Synthesis, FTIR, NMR (^{1}H and ^{13}C), UV–Vis spectra and Crystallographic data*
Data acquisition format	*CIF for Crystallography*
Data type	*Analyzed*
Procedure	*The compound* $C_{14}H_{11}ClN_2O_3$, *was synthesized and yellow block shaped single crystals were obtained. A single crystal of dimension 0.27× 0.26× 0.25mm^3 of the title compound are selected and X –ray intensity data was collected with different settings of ω and φ scan modes on a Bruker SMART APEXII CCD diffractometer using MoKα radiation (λ = 0.71073Å). Data Collection was performed by using the APEX2 software, whereas the cell refinement and data reduction were performed under the SAINT plus software. The crystal structure was solved by direct methods using the program SHELXS –2017 and refined by full–matrix least squares technique on F^2 using an isotropic displacement parameters using SHELXL –2017 program.*
Data accessibility	*Crystallographic data for the structure reported in this paper have been deposited with the Cambridge Crystallographic Data Centre supplementary publication no. CCDC 1562374. URL: https://summary.ccdc.cam.ac.uk/structure –summary –form*

1. Rationale

Schiff bases obtained from the condensation reaction of aldehydes with benzohydrazides have been widely investigated, either for their structures or for their biological properties [1 –5]. Important uses of hydrazones as plasticizers and stabilizers for polymers, polymerization initiators, antioxidants and as indicators were reported [6 –13].

Non-covalent bond interactions play an essential role in supramolecular architectures [14–18]. It is interactions between the molecules are weak intermolecular contacts that play a pivotal role in biological systems in the condensed phase [19–22]. Noncovalent binding interactions are now-a- days commonly used for the self-assembly of large supramolecular aggregates in solution with specific chemical properties [23]. Supramolecular interactions of aromatic systems have attracted considerable attention during the past decades [24,25], because of the utilization of intermolecular noncovalent interactions is relied upon for the design and development of novel functional materials [26, 27].

Structural conformations and density functional study of 2,4–dihydroxy –*N′* –(4 –methoxy benzylidene) benzohydrazide have been reported by Suresh et al. [28]. Our previous works on hydrazide derivatives have been reported [29–30]. In recent years, density functional theory (DFT) has been favourite in theoretical modelling. A literature search shows that the DFT has a great accuracy in reproducing the experimental values of in geometry [31–36].

Based on the previous researches and findings, attempts were made to continue our on–going studies on hydrazones. A report on X–ray crystal structure, Hirshfeld surface analysis, DFT and electronic properties of the title compound is done. Besides the single crystal XRD technique, the title compound is analyzed spectroscopic (FTIR, UV–Vis, ^{1}H and ^{13}C NMR) and DFT studies were made extensively. The HOMO-LUMO energy gap, NBO analysis and molecular electronic properties have also been computed. Analysis of intermolecular interactions using Hirshfeld surface-based tools represents a major advance in enabling supramolecular chemist to gain insight into crystal packing behaviour.

2. Procedure

2.1 Materials and methods

All the chemicals used in the synthesis were purchased from the Lancaster Chemical Company (UK), which is of spectroscopic grade and used without further purifications. Melting point was determination using the micro controller CL725 based digital melting point apparatus and temperature was recorded in °C. The FT–IR spectrum of compound was measured on a BRUKER IFS–66V spectrophotometer in the region 4000–400 cm^{-1} at a resolution of ±1 cm^{-1} by using KBr pellet. ^{1}H and ^{13}C NMR spectra were recorded on a 300 MHz AVANCE II (Bruker) spectrophotometer in DMSO–d^{6}. UV–Vis spectrum was obtained with a CARY/5E/UV spectrophotometer.

2.2 Synthesis of (E)–4–chloro–N'–(2,4–dihydroxy–benzylidene)benzohydrazide

An ethanolic solution (20ml) of 4–chlorobenzoic hydrazide (85mg) was added to the ethanolic solution (20ml) of 2,4–dihydroxy benzaldehyde (69mg). The reaction mixture was heated at 316 K for half an hour with constant stirring (Scheme 1). After air cooling, the reaction mixture was filtered and kept for crystallization. After a period of six days yellow coloured blocks shaped crystal of the title compound was obtained. The coloured crystal suitable for single crystal diffraction study was isolated. The melting point of the Schiff base was found to be 158°C. IR (KBr, cm^{-1}): The stretching vibrations are found at 3494, 3342 (O–H), 3260 (N–H), 1661(C=O), 1657 (C=N), 1330, 1297 (C–O), 1256 (C–N), 1119 (N–N) and 643 (C–Cl) respectively; ^{1}H NMR (DMSO–d6) δ (ppm): 11.98 (b,1H, OH), 11.40 (b,1H, OH), 8.51 (s, 1H, CH), 9.99 (NH), 7.96–7.31 (m, 3H, Ar –H), 6.38–6.32 (m, 4H, Ar–H); ^{13}C NMR (DMSO–d6) δ

(ppm): 161.91, 161.29, 159.98, 149.86, 132.19, 137.79, 132.19, 131.79, 129.94, 129.08, 110.97, 108.94 103.14. FT–IR, ^{1}H and ^{13}C NMR spectra of the title compound as shown in Figs. S1, S2 and S3 (Supporting information file).

2.3 X–ray structure analysis and refinement

A crystal with dimension of 0.27×0.26×0.25mm^3 was selected for X–ray data collection. All measurements were made on a BRUKER SMART APEXII CCD area–detector diffractometer with graphite monochromated MoKα (0.71073 Å) radiation, using ω and φ scan modes. Data Collection was performed by using the APEX2 software [37], whereas the cell refinement and data reduction were performed under the SAINT plus software [38]. The crystal structure was solved by direct methods and refined by full–matrix least squares technique on F^2 using SHELXS–2017 and SHELXL–2017 programs [38, 39]. The program ORTEP and PLATON [40] was exposing to view the molecular structures and to detect intramolecular and intermolecular hydrogen bonding interactions. All non hydrogen atoms were refined anisotropically and all the hydrogen atoms have been geometrically fixed and refined with isotropic thermal parameters. A summary of parameters for data collection and refinement is given in Table 1.

Supplementary crystallographic data were deposited in CCDC (Cambridge Crystallographic Data Centre, No: 1562374). The data can be obtained free of charge via http:/ www.ccdc.cam.ac.uk/ conts/retrieving.html, or e-mail: deposit@ccdc.ac.uk.

2.4 DFT calculations

Recently, the quantum chemical calculations were performed by Density functional theory (DFT) based on B3LYP/6–311G(d,p) basis set approximation in the GAUSSIAN 09W[41]. It was used to optimize molecular structure. Natural bond orbitals calculations were performed using NBO 3.1 program [42] as implemented in the GAUSSIAN 09W. The electrostatic potential surface and electronic properties were being recognized by DFT approach.

3. Data, value and validation

3.1 X–ray crystallography and molecular geometry

Single crystal X–ray analysis confirmed that the title compound was crystallized in the monoclinic crystal system, with $P2_1/c$ space group. The unit cell parameters for the compound are a =12.29 (2) Å, b = 9.724(15) Å, c = 12.43(2) Å, β = 114.86(2)° and Z= 4,V= 1389(4)Å^3. The asymmetric unit contains a molecule of a Schiff base. The dihedral angle between the benzene ring is 50.10(10)°. All the bond lengths are within normal ranges. The single crystal structure (ORTEP view) and optimized structure of the title compound along with numbering of atoms is shown in Fig.1. The optimized structural parameters of the title compound were

investigated by single crystal XRD and DFT-B3LYP/6–311G(d,p) method are presented in Table 2. The bond distances are O1–C7 =1.23(3), O2–C10=1.35(4) and O3–C12=1.36(3) Å in XRD values whereas the bond distances are O1–C7=1.21, O2–C10=1.37 and O3–C12=1.36Å in B3LYP for this title compound. The carbon–nitrogen bond lengths are also intermediate between C–N typical single (1.47 Å) and C=N double (1.27 Å) bonds [29, 30]. In the title compound**,** N–C bond lengths XRD values N1–C7 = 1.35(3) and N2–C8 = 1.28(3)Å are slightly shorter than N1–C7 = 1.38 and N2–C8 = 1.28 Å of B3LYP. In single crystal of the title compound, the hyrazide bond length is obtained at N1–N2 = 1.38(3)Å and 1.36Å in XRD and B3LYP method. The corresponding values obtained from X–ray diffraction pattern are also given in the Table 2 for comparison. From Table 2 it can be seen that there are small deviations in the computed geometric parameters from those obtained from the XRD data. These deviations can be attributed to the fact that the theoretical calculations have been carried out with isolated molecule in the gaseous phase and the experimental values correspond to molecule in the crystalline state. Also the change in the bond length of the C–H bond on substitution is due to a change in charge distribution on carbon atom of benzene ring. The two torsion angles τ1 (N–C–C–C) and τ2 (C–C–N–N) defines the confirmation of the molecule. In the present crystal structure, the torsion angles are observed at N1–N2–C8–C9 (–179.62° in XRD and –177.60° in DFT) and N2–C8–C9–C10 (–179.18°in XRD and –174.36° in DFT), N2–C8–C9–C14 (–0.82° in XRD and 7.27° in DFT) respectively.

Supramolecular features

In Schiff base compound, the molecular conformation is stabilized by an intramolecular O2–H2A···N2 hydrogen bond and intermolecular N1–H1···O2^{i}, O3–H4A···O1^{ii}, C2–H2···O3^{iii}, C11–H11···O1^{ii} bonds. In the compound, the intramolecular O—H···N hydrogen bond is formed between the OH group of 2, 4–dihydroxy phenyl derivative and N atom of azomethine moieties forming a ring motif with graph-set notation $R^2_2(24)$ and S(6) (Fig. 2). N1–H1···O2^{i} hydrogen bond is observed between the amide hydrogen (H1) and hydroxyl group (O2). Other hydroxyl group (O3) and O1 atom from carbonyl group interacts via O3–H4A···O1^{ii}, C11–H11···O1^{ii} and C2–H2···O3^{iii} hydrogen bonds forming a chain like arrangement along *a*-axis direction (Fig. 3). The hydrogen bonding geometries are shown in Table 3. The molecule is twisted rather than planar due to steric interaction between the central amide group and the two end groups. In addition, there are significant π–π stacking interactions [43–45]. In the crystal structure, stacking interactions are observed between the chlorophenyl moieties with a perpendicular separation of 3.336 Å, a centroid–to–centroid distance of 3.545 (2) Å and a slip angle (the angle between the centroid vector and the normal to the plane) of 19.78°.

3.3. UV–visible

The UV visible spectral peak at 301nm confirmed the presence of C=O group bonded system [46]. Absorption bands were observed at 331 nm and 242 nm (DMF) due to π–π* transitions of the aromatic rings and n–π* transitions of the C=N group respectively which also support the formation of Schiff base compound. It was found that the cut–off wavelength was at 351 nm and there was no absorption in the visible region due to the absence of any over tones and absorbance due to electronic transitions above 351 nm [47,48]. The absence of absorption in the entire visible region is sufficient for the second harmonic generation light (λ = 532 nm) from the Nd:YAG laser (λ=1064 nm), which is an essential parameter for NLO materials [49]. As a result it can be used as a potential material for SHG in the visible region. The UV visible spectrum is shown in Fig. 4.

4. Hirshfeld surface and electrostatic potential surface analysis

Hirshfeld surfaces [50–52] and the associated 2D-fingerprint [53–55] plots were calculated using *CrystalExplorer 3.1* [56], which accepts a structure input file in CIF format. Bond lengths to hydrogen atoms were set to typical neutron values (C–H = 1.083 A, N–H =1.009 A). For each point on the Hirshfeld isosurface, two distances d_e, the distance from the point to the nearest nucleus external to the surface, and d_i, the distance to the nearest nucleus internal to the surface, are defined. The normalized contact distance (d_{norm}) based on d_e and d_i is given by

$$d_{norm} = \frac{d_i - r_i^{vdw}}{r_i^{vdw}} + \frac{d_e - r_e^{vdw}}{r_e^{vdw}}$$

where r_i^{vdW} and r_e^{vdW} are the van der Waals radii of the atoms. The parameter d_{norm} displays a surface with a red-white-blue colour scheme, where bright red spots highlight shorter contacts, white areas represent contacts around the van der Waals separation, and blue regions are devoid of close contacts. The 3D d_{norm} surface of the title compound was shown in Fig. 5. The red points represent closer contacts and negative d_{norm} values on the surface corresponding to the N—H···O interactions, while C—H···O interactions are light red in colour.

The intermolecular interactions of the title compound are shown in the 2D fingerprint plots from Hirshfeld surface analyses are shown in Fig.6. This analysis identified the various intermolecular contacts (O–H, H–H, C–H, C–C, N–H, C–Cl, C–O, N–O, N–N and C–N) and their relative contributions in the crystal structure. The percentage of contacts that contribute to the total Hirshfeld surface are as follows: H···H (25.2%), O···H/H···O (23.2%), C···H/H···C (22.1%), C···C (5.8%), N···H/H···N(3.7%), C···O/O···C (1.8%), Cl···O/O···Cl (1.8%),

C···Cl/Cl···C (1.8%) C···N/N··· C (0.7%), N···O/ O···N (0.4%) and N···N(0.3%) are displayed in Fig. 6.

The molecular electrostatic potential is a physical property of a molecule can be defined in terms of total charge distribution of the molecule. A portion of a molecule that has a negative electrostatic potential is susceptible to an electrophilic attack – the more negative the better [57 – 59]. It provides a medium to understand the electron density which is useful for determining the electrophilic reactivity and nucleophilic reactivity as well as hydrogen –bonding interactions [60,58]. The different values of the electrostatic potential at the surface are represented by different colours; red and blue areas refer to the regions of negative and positive potentials and corresponding to the electron–rich and electron–poor regions, whereas the green colour signifies the natural electrostatic potential. The electrostatic potential is mapped on Hirshfeld surfaces using DFT (B3LYP/6–311G (d,p)) theory over the range of –7.184 a.u to –7.184 a.u. as shown in Fig.5. The electrostatic potential surfaces are plotted with red region, which is a negative (hydrogen acceptors) and blue region, which is a positive (hydrogen donor) [61]. It is seen that a region of zero potential envelopes the π–system of the benzene rings, leaving a more electrophilic region in the plane of the hydrogen atoms. These surfaces at sites close to the polar carbonyl group and the hydrazide group in the molecule show regions of most negative electrostatic potential and high activity of the carbonyl and hydrazide group. In contrast, regions close to the other polar atoms – oxygen of the phenyl ring show regions of slightly negative potential, whereas the other regions seem to present almost neutral potential as represented by the green region.

3.5 Frontier molecular orbitals

The electronic structure of the of the title compound in the gas phase has been calculated B3LYP/6–311G(d,p) method. The basic electronic parameters related to the orbitals in a molecule are the HOMO, LUMO and their resulting energy gap. These orbitals not only determine the way the molecule interacts with other species but their energy gap (HOMO – LUMO) helps to characterize the chemical reactivity and kinetic stability of the molecule [57 – 59]. Both the highest occupied molecular orbital (HOMO) and the lowest unoccupied molecular orbital (LUMO) are the main orbital take part in chemical stability [57–59]. Using Koopman's theorem [62,63] for closed–shell molecules, in the present study, the directly calculated HOMO and LUMO energies, the energy gap (ΔE), ionization potential (I), electron affinity (A), absolute electronegativity ($\chi = \frac{(I + A)}{2}$), absolute hardness ($\eta = \frac{(I - A)}{2}$) and electrophilicity index (

$\omega = \frac{\mu^2}{2\eta}$) and maximum charge transfer ($\Delta N_{max} = -\frac{\mu}{\eta}$) of the title compound were computed by B3LYP/6–311G(d,p) and listed in Table 4. Frontier orbital energy gap is generally the lowest energy electronic excitation that is possible in the title molecule. The value of the energy gap between HOMO and LUMO is 4.09eV, which is responsible for the bioactive property of the title compound is presented in Fig.7. The HOMO is found to be concentrated mainly over the N atom site and around its surrounding groups, but the LUMO lies mainly over the benzene ring.

3.6 NBO analysis

We have carried out natural bond orbital analysis to perform various second –order interactions between the filled orbitals of one subsystem and vacant orbitals of another subsystem, which is a measure of the intermolecular delocalization or hyper conjugation. The second order Fock matrix was carried out to evaluate the donor –acceptor interactions in the NBO analysis [64]. The interaction stabilization energy (E^2) that resulted from the second –order perturbation theory is reported in Table 5.

The larger the $E^{(2)}$ value, the stronger is the interaction between electron donors and electron acceptors, reveals a more donating tendency from electron donors to electron acceptors and a greater degree of conjugation of the whole system. Delocalization of the electron density between occupied Lewis type (bond or lone pair) NBO orbitals and formally unoccupied (antibond and Rydgberg) non Lewis NBO orbitals correspond to a stabilizing donor–acceptor interaction [65]. It is evident from Table 5, the important intra–molecular interactions are due to the orbital overlap between bonding (C–C) with the antibonding (C–C), and LP* chlorine orbitals.

The NBO analysis showed that in the title compound intra –molecular charge transfer from π(C1–C6) to π*(C2–C3), π*(C4–C5) and π(C2–C3) to π*(C1–C6), π*(C4–C5) and π(C4–C5)to π*(C1–C6), π*(C2–C3) leads to a large stabilization energy of 40.15, 40.54 kJ/mol and 40.14,47.78 kJ/mol and 42.50, 35.30 kJ/mol respectively. Charge transfer from LP(2) to σ*(C1–C7), σ*(C7–N14), π*(C20–C21) and π*(C22–C23) involves the stabilization energy of 26.69, 41.53, 42.47 and 44.02 kJ/mol respectively. These interactions lead to an increase in electron density in C1–C6 and C4–C5 anti bonding orbitals that weakens the respective bonds.

3.7 Nonlinear optical effects

Molecules that show asymmetric polarization induced by electron donor and acceptor groups in π – electron conjugated molecules are good candidates for nonlinear optical (NLO) applications in optical signal processing, telecommunications and optical computing [66–70]. In the present study NLO behaviour of the title compound was investigated by the determination of

the hyperpolarizability (β), electric dipole moment (μ) and the polarizability (α) by using the B3LYP/6 –311G(d, p) basis set. The calculated values are listed in Table 6.

The criteria for a molecule to behave as a good NLO, it should have a large value of the first hyperpolarizability (β). In presence of an applied electric field, the energy of a system is a function of the electric field. The first hyperpolarizability is a third rank tensor that can be described by a 3×3×3 matrix. The 27 components of the matrix can be reduced to 10 components due to the Kleinman symmetry [71]. The components of β are defined as the coefficients in the Taylor series expansion of the energy in the external electric field. When the electric field is weak and homogeneous, this expansion becomes

$$E = E_0 - \mu_i F_i - 1/2\ \alpha_{ij} F_i F_j - 1/6\ \beta_{ijk} F_i F_j F_k + \ldots$$

where E_0 is the energy of the unperturbed molecules, F_i is the field at the origin μ_i, α_{ij} and β_{ijk} are the components of dipole moment, polarizability, and the first hyperpolarizability, respectively. The total electric dipole moment (μ), the mean polarizability <α>, and the total first order hyperpolarizability (β), have been calculated using the *x*, *y*, and *z* components of these electric moments. Urea is used as a reference for the characterization of organic nonlinear materials. The computed value of (β) is 20.073×10^{-30} e.s.u. obtained by DFT (B3LYP)/6–311G (d,p) method for the title compound. These are greater than those of urea (β = 0.37289 x 10^{-30} e.s.u). The first order hyperpolarizability of the title compound is 53 times greater than that of urea and thus it could be a potential NLO molecule for future studies. The calculated total static dipole moment of the title compound was 1.8784 Debye.

Conclusion

The (*E*)–4–chloro–*N*'–(2,4–dihydroxy–benzylidene)benzohydrazide was synthesized and characterized by means of various spectroscopic tools like: FTIR, ^{1}H NMR, ^{13}C NMR, UV-Vis spectra and finally the three dimensional structure of the title compound was confirmed by single crystal X-ray diffraction studies. The optimized structural parameters were investigated by single crystal XRD and B3LYP/6–311G(d,p) method. The optimized geometric parameters results show good concurrence with the XRD values. The crystal and molecular structure of the title compound is stabilized by an intramolecular O—H···N hydrogen bond and intermolecular N—H···O, O—H···O, C—H···O, C—H···O hydrogen bonds. The optical behaviour was evaluated by UV–Vis analyses showed that the title compound can be utilized for NLO applications and Photonic device fabrications; this is supported by the hyperpolarizability value obtained by DFT calculations. The various intramolecular interactions that is responsible for the stabilization of the molecule was revealed by natural bond orbital analysis.

Further, three dimensional d_{norm} and 2D fingerprint plots for the title compound were studied extensively to understand the intermolecular interactions. The title compound disclosed that H···H (25.2%) interactions has maximum contribution to the total Hirshfeld surface. Other electronic structure properties such as HOMO-LUMO analysis, ionization potential, electron affinity, absolute electronegativity, hardness, electrophilicity index and maximum charge transfer of the title compound were done.

Acknowledgements

AGA thanks the University Grants Commission (UGC) for the award of a Research Fellowship under the Faculty Development Programme (FDP). The authors are thankful to the Institution of Excellence, Vijnana Bhavana, University of Mysore, Mysuru, for providing the single–crystal X–ray diffraction facility.

References

[1] H. K.Fun, P. S. Patil, S. R. Jebas, K. V. Sujith, B. Kalluraya, 4-Chloro-N'-[(Z)-4-(dimethylamino)benzylidene]benzohydrazide monohydrate, ActaCryst. E64 (2008) o1594.

[2] A. A. Alhadi, H.M. Ali, S. Puvaneswar, W. T. Robinson, S.W. Ng, N′-(5-Bromo-2-hydroxybenzylidene)-3,4,5-trihydroxybenzohydrazide dehydrate, ActaCryst. E64 (2008) o1584.

[3] H. M. Ali, K. Zuraini, B. Wan Jefrey, S. W. Ng, N′-(2-Chloro-5-nitrobenzylidene)-3-hydroxybenzohydrazide methanol solvate, ActaCryst. E63 (2007) o1729.

[4] Jiu-Fu Lu, Suo-Tian Min, Xiao-Hui Ji, Zhong-Hai Dang, N′-(2-Hydroxybenzylidene)-2-methoxybenzohydrazide monohydrate, ActaCryst. E64 (2008) o1693.

[5] S. Shan, Y. L. Tian, S. H. Wang, W. L. Wang, Y. L. Xu, (E)-N'-[1-(4-Amino-phen-yl)ethyl-idene]benzohydrazide, ActaCryst. E64 (2008) o1363.

[6] G. Strappaghetti, C.Brodi, G. Giannaccini, L. Betti,New 4-(4-methyl-phenyl) phthalazin- (2H)-one derivatives and their effects on α_1-receptors, Bioorg. Med. Chem. Lett. 16 (2006) 2575–2579

[7] F. Al–Assar, K. N. Zelenin, E. E. Lesiovskaya, I. P. Bezant & B. A.Chakchir, Synthesis and pharmacological activity of 1-hydroxy-, 1-amino-, and 1-hydrazino-substituted 2,3-dihydro-1h-pyrazolo[1,2-a]pyridazine-5,8-diones and 2,3-dihydro-1h-pyrazolo[1,2-b] phthalazine-5,10-diones , J. Pharm. Chem. 36 (2002) 598–603.

[8] F. A. O. Adekunle, J. A. O. Woods, O. A. Odunola, Synthesis, Physicochemical and Biological Studies of Cobalt(II) and Copper(II) Complexes of Benzoylacetic Acid Hydrazide Res, J. Pharm. Bio. Chem. Sci. 3 (2012)1120–1127.

[9] R. P. Jain, J. C. Vederas, Structural Variations in Keto Glutamines for Improved Inhibition against Hepatitis A Virus 3C Proteinase, Bioorg. Med. Chem. Lett. 14 (2004) 3655–3658.

[10] T. Jeeworth, H. L. K.Wah, M. G. Bhowon, D. Ghoorhoo, K.Babooram, Synthesis and anti-bacterial/catalytic properties of schiff bases and schiff base metal complexes derived from 2,3-diaminopyridine, Synth. React. Inorg. Met.Org. Chem. 30 (2000) 1023–1038.

[11] A. Scozzafava, L. Menabuoni, F. Mincione, G.Mincione, C. T. Supuran, Carbonic anhydrase inhibitors: Synthesis of sulfonamides incorporating dtpa tails and of their zinc complexes with powerful topical antiglaucoma properties, Bioorg. Med. Chem. Lett. 11 (2001) 575–582.

[12] Nora H. Al-Sha'alan, Antimicrobial Activity and Spectral, Magnetic and Thermal Studies of Some Transition Metal Complexes of a Schiff Base Hydrazone Containing a

Quinoline Moiety, Molecules 12 (2007) 1080–1091.

[13] K. Siddappa, T.Reddy ,M. Mallikarjun, C. V. Reddy, Synthesis, characterization and antimicrobial studies of 3-[(2-hydroxy-quinolin-3-ylmethylene)-amino]-2-phenyl-3H-quinazolin-4-one and its metal(II) complexes, Eur. J. Chem.5 (2008) 155–162.

[14] J. M. Lehn, Supramolecular Chemistry-Concepts and Perspectives; VCH: Weinheim, Germany (1995).

[15] M. Fujita, Molecular Self-Assembly Organic versus Inorganic Approaches, Struct. Bonding (Berlin), Springer-Verlag; Berlin: Germany, Vol. 96 (2000).

[16] S. L. R. MacGillivray, J. L. Atwood, $[Cu(C_{12}N_2H_8)_2(C_2H_3O_2)][B_5O_6(OH)_4]\cdot C_4H_9NO$: First Borate with Three-dimensional Supramolecular Framework Formed by Hydrogen Bonds and π···π Stacking Interactions, Nature 389 (1997) 469–472

[17] K. Biradha, M. J. Zaworotko, A Supramolecular Analogue of Cyclohexane Sustained by Aromatic C-H···π Interactions: Complexes of 1,3,5-trihydroxybenzene with Substituted Pyridines, J. Am. Chem. Soc. 120(1998) 6431–6432.

[18] S. K. Seth, I. Saha, C. Estarellas, A. Frontera, T. Kar, S. Mukhopadhyay, Supramolecular Self-Assembly of M-IDA Complexes Involving Lone-Pair•••π Interactions: Crystal Structures, Hirshfeld Surface Analysis, and DFT Calculations [H2IDA=iminodiacetic acid, M = Cu(II), Ni(II)], Cryst. Growth Des. 11(2011) 3250–3265.

[19] L. J. Childs, N. W. Alcock, M. Hannon, Assembly of nano-scale circular supramolecular arrays through π-π aggregation of arc-shaped helicate units, Angew. Chem., Int. Ed. 40 (2001)1079–1081.

[20] A. D. Bond, C–H···π interactions in the low-temperature crystal structures of α, ω-unsaturated linear hydrocarbons, Chem. Commun. (2002) 1664–1665.

[21] M. Kidowaki, N. Tamaoki, Inorganic–organic hybrid photochromic materials, Chem. Commun. (2003) 290–291.

[22] G. R. Desiraju, Crystal Engineering: The Design of Organic Solids; Elsevier Science Publishers B. V.: Amsterdam, The Netherlands (1989).

[23] D. T. Bowron, J. L. Finney, A. K. J. Soper, J. Am. Chem. Soc. 128(2006) 5119–5126.

[24] D. N. Reinhoudt, M. Crego-Calama, Synthesis Beyond the Molecule, Science 295 (2002) 2403–2407.

[25] A. L. Maksimov, D. A. Sakharov, T. Y. Filippova, A. Y. Zhuchkova, E. A. Karakhanov, Supramolecular catalysts on the basis of molecules-receptors, Ind. Eng. Chem. Res. 44 (2005) 8644–8653.

[26] J.W. Bell, N.M. Hext, Supramolecular optical chemosensors for organic analytes, Chem. Soc. Rev. 33 (2004) 589–598.

[27] C. J. Janiak, A critical account on $\pi - \pi$ stacking in metal complexes with aromatic nitrogen-containing ligands, J. Chem. Soc. Dalton Trans. 21 (2000) 3885–3896.

[28] D. M. Suresh, D. Sajan, Y. P. Diao, I. Němec, I. Hubert Joe, V. Bena Jothy, Structural conformations and density functional study on the intramolecular charge transfer based on vibrational spectra of 2,4-dihydroxy-N'-(4-methoxybenzylidene) benzo hydrazide, Spectrochimi. Acta A 110 (2013) 157–168.

[29] C. Arunagiri, A. G. Anitha, A. Subashini, S. Selvakumar, Synthesis, X-ray crystal structure, vibrational spectroscopy, DFT calculations, electronic properties and Hirshfeld analysis of (E)-4-Bromo-N'-(2,4-dihydroxy-benzylidene) benzohydrazide, Journal of Molecular Structure 1163 (2018) 368–378.

[30] C. Arunagiri, A. G. Anitha, A. Subashini, S. Selvakumar, N. K. Lokanath, Synthesis, single crystal, structure and Hirshfeld surface analysis of (E)–4–toluic –N'–(2, 4–dihydroxy–benzylidene) benzohydrazide, Chemical Data Collections 17–18 (2018) 169–177.

[31] G. Fitzgerald and J. Andzelm, Chemical Applications of Density Functional Theory: Comparison to Experiment, Hartree-Fock and Perturbation Theory, J. Phys. Chem. 95(1991) 10531–10534.

[32] T. Ziegler, Density functional theory as a practical tool for the study of elementary reaction steps in organometallic chemistry, Pure Appl. Chem. 63(1991) 873–878.

[33] J. Andzelem, E. Wimmer, Density functional Gaussian-type-orbital approach to molecular geometries, vibrations, and reaction energies, J. Chem. Phys. 95 (1992) 1280–1303.

[34] G. E. Scuseria, Comparison of coupled cluster results with a hybrid of Hartree–Fock and density functional theory, J. Chem. Phys.97 (1992) 7528–7530.

[35] R. M. Dickson and A. D. Becke, Basis-set-free local density-functional calculations of geometries of polyatomic molecules, J. Chem. Phys. 99 (1993) 3898–3902.

[36] S. Seth, D. Sarkarc, T. Kar, Use of $\pi - \pi$ forces to steer the assembly of chromone derivatives into hydrogen bonded supramolecular layers: crystal structures and Hirshfeld surface analyses, CrystEngComm.13(14) (2011) 4528–4532.

[37] Bruker. APEX2, SADABS and SAINT–Plus. Bruker AXS Inc., Madison, Wisconsin, USA (2013).

[38] G. M. Sheldrick, Crystal structure refinement with SHELXL, Acta Cryst. A71 (2015)

3–8.

[39] G. M. Sheldrick, SHELX2017, Programs for crystal structure determination, Universität Göttingen, Germany (2017).

[40] A. L. Spek, Structure validation in chemical crystallography, Acta Cryst. D65 (2009) 148–155.

[41] M.J. Frisch et al., Gaussian Inc., Wallingford, CT (2009).

[42] E.D. Glendening, A.E. Reed, J.E. Carpenter, F. Weinhold, NBO Version 3.1,Gaussian Inc., Pittsburgh, PA(2003).

[43] S. Seth , P. Manna, N. J. Singh, M. Mitra, A.D. Jana, A. Das, S. R. Choudhury, T. Kar, S.Mukhopadhyay, K. S. Kim, Molecular architecture using novel types of noncovalent π -interactions involving aromatic neutrals, aromatic cations and π -anions, CrystEngComm. 15(7) (2013) 1285–1288.

[44] P. Manna, S. K. Seth, M. Mitra, A. Das, N.J. Singh, S. R. Choudhury, T. Kar, Mukhopadhyay, A successive layer-by-layer assembly of supramolecular frameworks driven by a novel type of face-to-face $\pi^+ - \pi^+$ interactions, CrystEngComm.15 (39) (2013) 7879–7886.

[45] C. A. Hunter, Meldola Lecture. The role of aromatic interactions in molecular recognition, Chem. Soc. Rev. 23(1994) 101–109.

[46] A. Furniss, B. Hannaford, C. Smith, D. Tatchell, Vogel's Text book of practical organic chemistry, ELBS 5th edition (1989).

[47] L. Caroline, S. Vasudevan, Growth and characterization of L-phenylalanine nitric acid, a new organic nonlinear optical material, Mater. Lett. 63 (2009) 41–44.

[48] A. Antony Joseph, I. John David Ebenezar, C. Ramachandra Raja, Crystal growth, spectral and NMR studies of nonlinear optical crystal: L-valinium picrate, Optik 123 (2012) 1436–1439.

[49] V.Krishnakumar, R. NagaLakshmi, Polarised infrared and Raman studiesof YCa4O(BO3)3 a non-linear optical single crystal, Spectrochim. Acta A 60(12) (2004) 2733–2739.

[50] F. L. Hirshfeld, Synthesis, Crystal structure, and Hirshfeld Surface Analysis of a New Mixed Ligand Copper(II) Complex, Theor. Chim. Acta 44 (1977)129–138.

[51] H. F. Clausen, M. S. Chevallier, M. A. Spackman and B. B. Iversen, Three new co-crystals of hydroquinone: crystal structures and Hirshfeld surface analysis of intermolecular interactions, New J. Chem.34 (2010) 93–199.

[52] S. K. Seth, I. Saha, C. Estarellas, A. Frontera, T. Kar and S. Mukhopadhyay,

Supramolecular Self-Assembly of M-IDA Complexes Involving Lone-Pair···π Interactions: Crystal Structures, Hirshfeld Surface Analysis, and DFT Calculations [H_2IDA = iminodiacetic acid, M = Cu(II), Ni(II)] Cryst. Growth Des. 11(2011) 3250–3265.

[53] A. L. Rohl, M. Moret, W. Kaminsky, K. Claborn, J. J. McKinnon and B. Kahr, Hirshfeld Surfaces Identify Inadequacies in Computation of Intermolecular Interactions in Crystals: Pentamorphic 1,8-Dihydroxyanthraquinone, Cryst. Growth Des. 8 (2008) 4517–4525.

[54] A. Parkin, G. Barr, W. Dong, C. J. Gilmore,D. Jayatilaka, J. J. McKinnon, M. A. Spackman and C.C. Wilson, Comparing entire crystal structures: structural genetic fingerprinting, CrystEngComm. 9 (2007) 648–652.

[55] M.A. Spackman and J. J. McKinnon, Fingerprinting intermolecular interactions in molecular crystals, CrystEngComm. 4 (2002) 378–392.

[56] S. K. Wolff, D. J. Grimwood, J. J. McKinnon, M. J.Turner, D. Jayatilaka, M. A. Spackman, University of Western Australia, CrystalExplorer (Version 3.1) (2012).

[57] E. Scrocco, J. Tomasi, Topics in Current Chemistry, Vol. 7, Springer, Berlin, 1973.

[58] F.J. Luque, J.M. Lopez, M. Orozco, Perspective on "Electrostatic interactions of a solute with a continuum". A direct utilization of ab initio molecular potentials for the prevision of solvent effects, Theor. Chem. Acc. 103 (2000) 343–345.

[59] N. Okulik, A.H. Jubert, Theoretical Analysis of the Reactive Sites of Non–steroidal Anti–inflammatory Drugs, Internet Electron. J. Mol. Des. 4 (2005) 17–30.

[60] S. Sebastin, N. Sundaraganesan, The spectroscopic (FT-IR, FT-IR gas phase, FT-Raman and UV) and NBO analysis of 4-Hydroxypiperidine by density functional method. Spectrochim. Acta A75(2010) 941–952.

[61] S. M. Kumar, B. C. Manjunath, F. H. Al-Ostoot, M. Jyothi, M. Al-Ghorbani, S. A. Khanum, A. K. Kudva, N. K. Lokanath, K. Byrappa, Synthesis, crystal structure and Hirshfeld surfaces of 1-(3,4-dimethoxyphenyl)-3-(3-hydroxyphenyl) prop-2-en-1-one, Chemical Data Collections 15-16 (2018)153–160.

[62] T. Koopmans, Über die Zuordnung von Wellenfunktionen und Eigenwerten zu den Einzelnen Elektronen Eines Atoms, Physica 1 (1933) 104–113.

[63] B. Gomez, N.V. Likhanova, M. A.Dominguez-Aguilar, R. Martinez-Palou, A. Vela Quantum Chemical Study of the Inhibitive Properties of 2-Pyridyl-Azoles, J. Gasquez, J. Phy. Chem. B110 (2006) 8928–8934.

[64] M. Szafram, A. Komasa, E.B. Adamska, A combined experimental and theoretical

approach for structural, spectroscopic, NLO, NBO, thermal and photophysical studies of new fluorescent 5-amino-1-(7-chloroquinolin-4-yl)-1H-1,2,3-triazole-4-carbonitrile using density functional theory, J. Mol. Struct. 827 (2007) 101–107.

[65] J. Zyss, J.F. Nicoud, Status and perspective for molecular nonlinear optics: from crystals to polymers and fundamentals to applications, Curr. Opin. Solid State Mater. Sci. 1 (1996) 533–546.

[66] R. Dagani, Devices based on electro-optic polymers begin to enter marketplace, Chem. Eng. News. 74(10)(1996) 22–27.

[67] D. M. Boyd, M. G. Kuzyk, Polymers for Electronic and Photonic Applications; (Academic Press: New York, 1993).

[68] N. Peyghambarian, S. W. Koch, A. Mysyrowicz, Introduction to Semiconductor Optics; (Prentice Hall: Englewood Cliffs, 1993).

[69] T. Kiano, S. Tomaru, Organic materials for nonlinear optics, Adv. Mater. 5(1993) 172–178.

[70] S. R Marder, J. W. Perry, Nonlinear Optical Polymers: Discovery to Market in 10 Years, Science 263(1994) 1706–1707.

[71] D. A. Kleinman, Nonlinear Dielectric Polarization in Optical Media, Phys. Rev.126 (1962) 1977–1979.

Table 1

Crystal data and structure refinement parameters of the title compound.

CCDC deposit No.	1562374
Crystal data Formula	$C_{14}H_{11}ClN_2O_3$
Formula weight	290.70
Crystal system	monoclinic
Space group	$P2_1/c$
a,b,c [Å]	12.29 (2), 9.724 (15), 12.43 (2)
α, β, ν [˚]	90.00 (2), 114.86 (2), 90.00 (2)
V[$Å^3$]	1348 (4)
Z	4
D(calc)[Mg/m^3]	1.433
μ(Mo Kα) [$/mm^{-1}$]	0.29
F(000)	600
Crystal size [mm]	0.27, 0.26, 0.25
θ Min–Max [˚]	3.3 – 27.5
Dataset	−12→15: −12→10: −14→16
Temperature (K)	293
Radiation [Å]	MoKα 0.71073
Nref, Npar	3030, 181
R, wR2, S	0.051, 0.145, 1.03
Largest diff. peak and hole ($e/Å^{-3}$)	0.34, −0.33

Table 2

Theoretical and experimental structural geometry parameters of bond lengths (Å), bond angles (°) and torsion angles (°) involving the non-hydrogen atoms for the title compound.

Bond lengths (Å)	DFT	XRD	Bond angles (°)	DFT	XRD	Torsion angles (°)	DFT	XRD
Cl1 – C1	1.76	1.74	C2–C1–C6	118.87	119.07	C6–C1–C2–C3	–1.69	–0.96
O1 – C7	1.21	1.23	C2–C1–C7	117.05	119.20	C7–C1–C2–C3	–179.25	–177.96
O2 – C10	1.37	1.35	C6–C1–C7	124.03	122.66	C2–C1–C6–C5	1.26	0.10
O3 – C12	1.36	1.36	C1–C2–C3	120.92	121.01	C7–C1–C6–C5	178.64	176.96
N1– C7	1.38	1.35	C2–C3–C4	119.09	118.61	C2–C1–C7–O1	23.42	28.25
N1– N2	1.36	1.38	C3–C4–C5	121.20	121.82	C2–C1–C7–N1	–155.90	–151.52
N2 – C8	1.28	1.28	C3–C4–Cl1	119.45	119.73	C6–C1–C7–O1	–154.00	–148.63
C1 – C6	1.40	1.37	C5–C4–Cl1	119.35	118.44	C6–C1–C7–N1	26.67	31.61
C1 – C2	1.40	1.37	C4–C5–C6	119.07	119.45	C1–C2–C3–C4	0.88	0.93
C2 – C3	1.39	1.38	C1–C6–C5	120.82	120.02	C2–C3–C4–C5	0.39	–0.04
C3 – C4	1.39	1.39	C1–C7–O1	122.17	121.41	C3–C4–C5–C6	–0.80	–0.80
C4 – C5	1.39	1.38	C1–C7–N1	114.18	115.36	Cl10–C4–C5–C6	179.73	179.76
C5 – C6	1.50	1.49	O1–C7–N1	123.64	123.23	C4–C5–C6–C1	–0.03	0.76
C1 – C7	1.39	1.38	C7–N1–N2	120.98	119.83	C4–C5–C6–C1	–0.03	0.76
C8 – C9	1.46	1.44	N1–N2–C8	116.84	116.02	O1–C7–N1–N2	2.31	3.09
C9 – C14	1.41	1.40	N1–C8–C9	121.42	121.54	C7–N1–N2–C8	–174.25	–169.46
C9 – C10	1.41	1.40	C8–C9–C10	120.33	122.61	N1–N2–C8–C9	–179.62	–177.60
C10 – C11	1.40	1.36	C8–C9–C14	121.94	119.91	N2–C8–C9–C10	179.18	–174.36
C11 – C12	1.40	1.39	C10–C9–C14	117.73	117.46	N2–C8–C9–C14	–0.82	7.27
C12– C13	1.39	1.38	C9–C10–C11	121.03	120.99	C8–C9–C10–C11	179.98	–179.04
C13 – C14	1.39	1.38	C9–C10–O2	117.54	117.31	C8–C9–C10–O2	–0.05	–1.55
			C11–C10–O2	121.43	121.70	C14–C9–C10–C11	–0.02	–0.59
			C10–C11–C12	119.85	119.76	C14–C9–C10–O2	179.95	–179.96
			C11–C12–C13	120.15	120.29	C8–C9–C14–C13	–179.99	178.00
			C11–C12–O3	117.09	118.24	C10–C9–C14–C13	0.003	–0.59
			C13–C12–O3	122.76	121.48	C9–C10–C11–C12	0.03	1.37
			C12–C13–C14	119.40	119.34	O2–C10–C11–C12	–179.94	–179.06
			C9–C14–C13	121.83	122.15	C10–C11–C12–C13	–0.024	–1.37
						C10–C11–C12–O3	179.99	178.41
						C11–C12–C13–C14	0.0082	0.39
						O3–C12–C13–C14	179.99	–179.39
						C12–C13–C14–C9	0.002	0.60

Table 3

Hydrogen-bond geometry (Å, °) of the title compound.

Bond D —H···A	Bond length (Å)			Bond angle (°)	Symmetry code
	D—H	H···A	D···A	D —H···A	
N(1) — H(1)···O(2)^{i}	0.86	2.18	2.994(5)	158	$x, -y-1/2, z-1/2$
O(3)—H(4A)···O(1)^{ii}	0.92(3)	1.78(3)	2.695(5)	175(3)	$-x+1, y-1/2, -z+3/2$
O(2)—H(2A)···N(2)	0.87(3)	1.88(2)	2.638(5)	144(2)	
C(2)—H(2)···O(3)^{iii}	0.93	2.59	3.501(6)	166	$-x+1, -y-1, -z+1$
C(11)— H(11)···O(1)^{ii}	0.93	2.56	3.221(6)	128	$-x+1, y-1/2, -z+3/2$

Table 4

Molecular properties of the title compound from orbital energies calculated by B3LYP/6–311G(d,p) method

Chemical parameters (in eV)	Values
E_{HOMO}	–5.8209
E_{LUMO}	–1.7287
$E_{HOMO\ –LUMO}$ gap (ΔE)	4.09
$E_{HOMO\ –1}$	–6.8546
E_{LUMO+1}	–1.0547
$E_{HOMO\ –1\ –LUMO+1}$ gap	5.80
Electronegativity (χ)	3.7748
Chemical hardness (η)	2.0461
Softness (ζ)	0.4887
Electrophilicity index(ω)	3.4820
Chemical Potential(μ)	–3.7748

Table 5

Selected second order perturbation theory analysis of Fock Matrix in NBO basis corresponding to the intra –molecular bonds of the title compound.

Donor (i)	Type	ED/e	Acceptor (j)	Type	ED/e	$E^{(2)a}$ ($kjmol^{-1}$)	E(j) –E(i)[b] (a.u)	F(i,j)[c] (a.u)
C1 –C6	π	1.665	C2 –C3	π *	0.291	41.15	0.49	0.129
C1 –C6	π	1.665	C4 –C5	π *	0.374	40.54	0.46	0.123
C2 –C3	π	1.644	C1 –C6	π *	0.366	40.14	0.46	0.122
C2 –C3	π	1.980	C4 –C5	π *	0.374	47.78	0.45	0.131
C4 –C5	π	1.676	C1 –C6	π*	0.366	42.50	0.49	0.131
C19 –C24	σ	1.971	C23 –C24	σ*	0.016	40.25	1.78	0.078
C19 –C24	π	1.659	N16 –C17	π*	0.135	25.32	0.49	0.105
C19 –C24	π	1.659	C20 –C21	π*	0.381	57.05	0.45	0.145
C19 –C24	π	1.659	C22 –C23	π*	0.395	27.46	0.45	0.101
C20 –C21	π	1.701	C19 –C24	π*	0.375	23.66	0.50	0.099
C20 –C21	π	1.701	C22 –C23	π*	0.395	53.95	0.48	0.148
C22 –C23	π	1.654	C19 –C24	π*	0.375	61.01	0.49	0.1555
C22 –C23	π	1.654	C20 –C21	σ*	0021	26.32	0.47	0.100
LP(2)	n	1.883	C1 –C7	σ*	0.057	26.69	1.06	0.152
LP(2)	n	1.883	C7 –N14	σ*	0.069	41.53	1.07	0.190
LP(1)	n	1.763	C7 –O13	π*	0.209	70.57	0.59	0.184
LP(1)	n	1.763	N16 –C17	π*	0.006	33.97	0.58	0.128
LP(2)	n	1.903	C20 –C21	π*	0.381	42.47	0.64	0.159
LP(2)	n	1.896	C22 –C23	π*	0.024	44.02	0.63	0.161
C1 –C6	π*	0.366	C2 –C3	π*	0.291	356.26	0.02	0.123
C1 –C6	π*	0.366	C7 –O13	π*	0.209	57.56	0.06	0.094
C4 –C5	π*	0.374	C1 –C6	π*	0.366	431.71	0.02	0.129
C4 –C5	π*	0.374	C2 –C3	π*	0.291	162.51	0.04	0.117
C19 –C24	π*	0.374	N16 –C17	π*	0.135	145.39	0.02	0.092
C20 –C21	π*	0.381	C19 –C24	π*	0.375	375.18	0.02	0.119
C22 –C23	π*	0.395	C19 –C24	π*	0.375	415.89	0.02	0.126

[a] $E^{(2)}$ means energy of hyperconjugative interactions (stabilization energy).
[b] Energy difference between donor and acceptor i and j NBO orbitals.
[c] F(i, j) is the Fock matrix element between i and j NBO orbitals.

Table 6

Calculated Dipole moment, Polarizability and hyperpolarizability for the title compound.

Dipole Moment (Debye)		**Hyper polarizability (a.u)**	
μ_x	1.4245	β_{xxx}	–2370.46
μ_y	0.7291	β_{xxy}	–53.4479
μ_z	–0.9836	β_{xyy}	71.4271
μ_{tot}	1.8784	β_{yyy}	–12.7919
Polarizability (a.u)		β_{xxz}	335.2324
α_{xx}	389.388	β_{xyz}	–63.0904
α_{yy}	–20.8073	β_{yyz}	12.2991
α_{zz}	109.501	β_{xzz}	12.941
α_{xy}	–1.6131	β_{yzz}	–14.1587
α_{xz}	–43.8902	β_{zzz}	0.5795
α_{yz}	160.6092	$\beta_{(Total)}$	2323.4769
α_{mean}	463.639	β (e.s.u)	20.073×10^{-30}
α(e.s.u)	0.6871×10^{-24}		

Figure captions

Scheme 1: Synthesis of Schiff base of the title compound.

Fig. 1: The ORTEP and optimized structure of the title compound.

Fig. 2: A hydrogen bonding (C2–H2···O3 and O2–H2A···N2) interactions of the title compound.

Fig. 3: A hydrogen bonding (N1–H1···O2, O3–H4A···O1 and C11–H11···O1) interactions of the title compound.

Fig. 4: UV-Vis spectrum of the title compound.

Fig. 5: d_{norm} mapped on Hirshfeld surface and molecular electrostatic potential mapped for visualizing the intermolecular contacts of the title compound.

Fig. 6 : Fingerprint plots of the title compound showing the overall contribution of the contacts to the surface.

Fig. 7: The atomic orbital compositions of the frontier molecular orbital of the title compound.

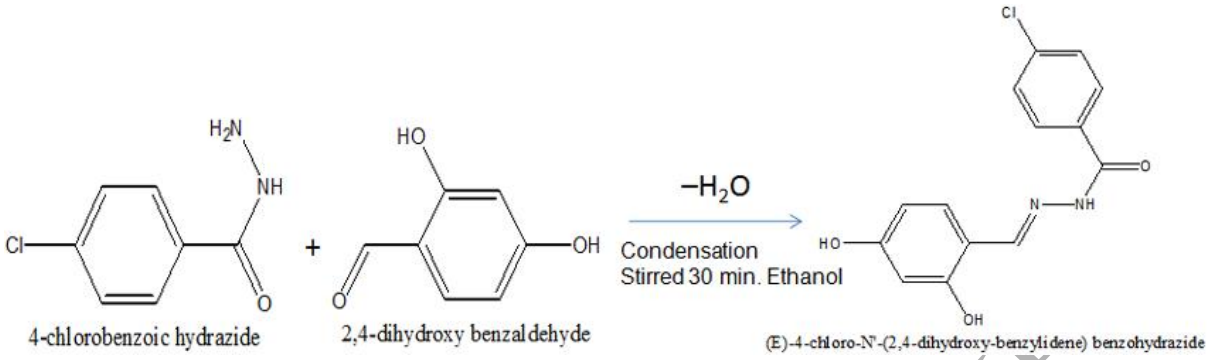

Scheme 1

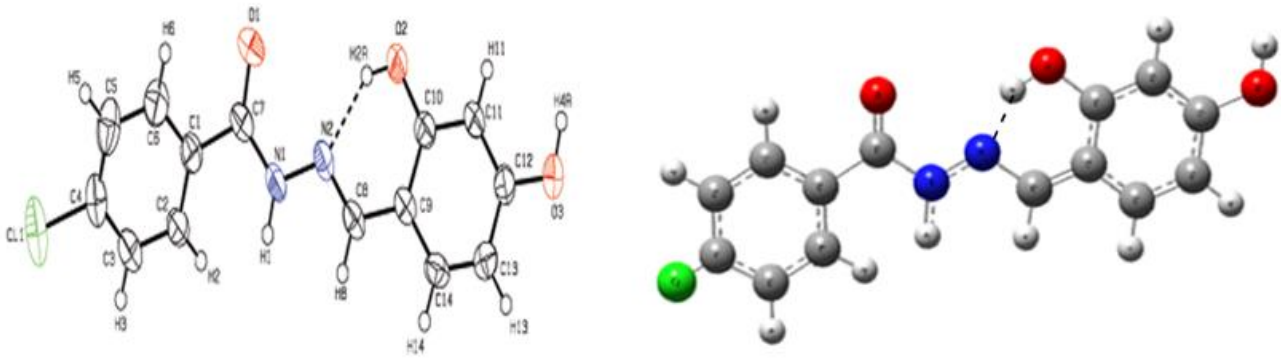

Fig. 1

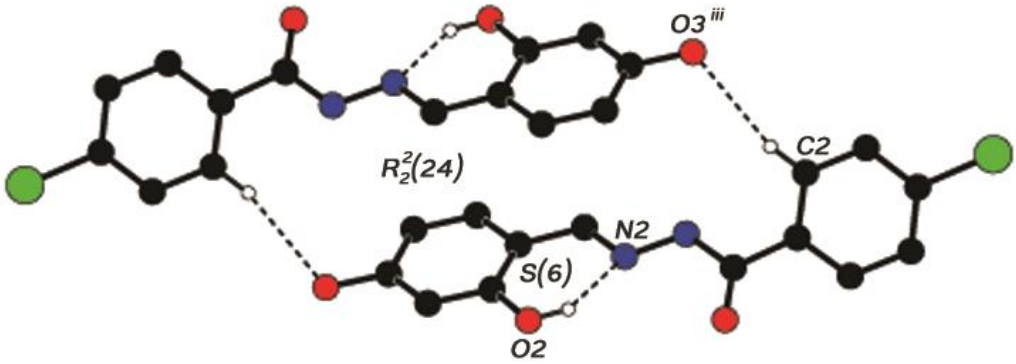

Fig. 2

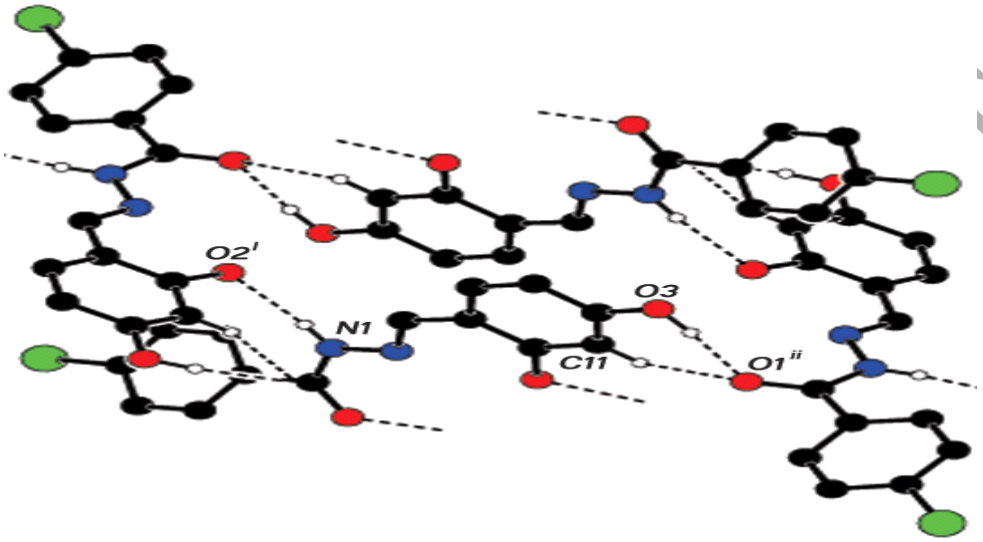

Fig. 3

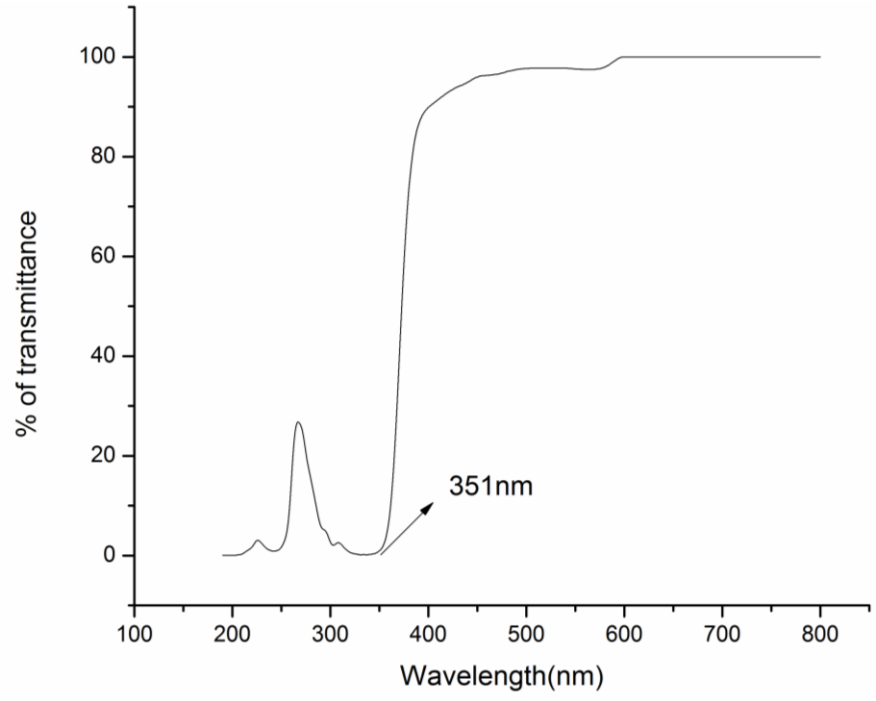

Fig. 4

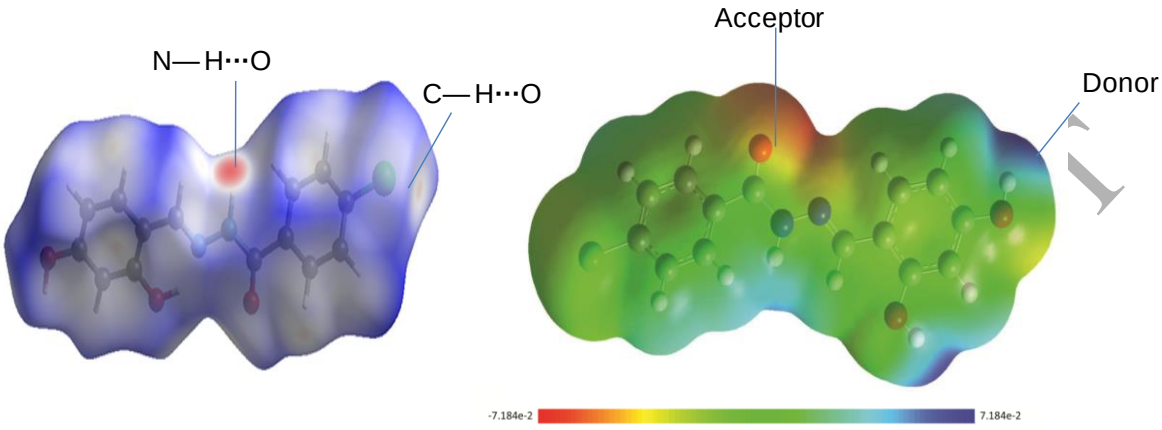

Fig. 5

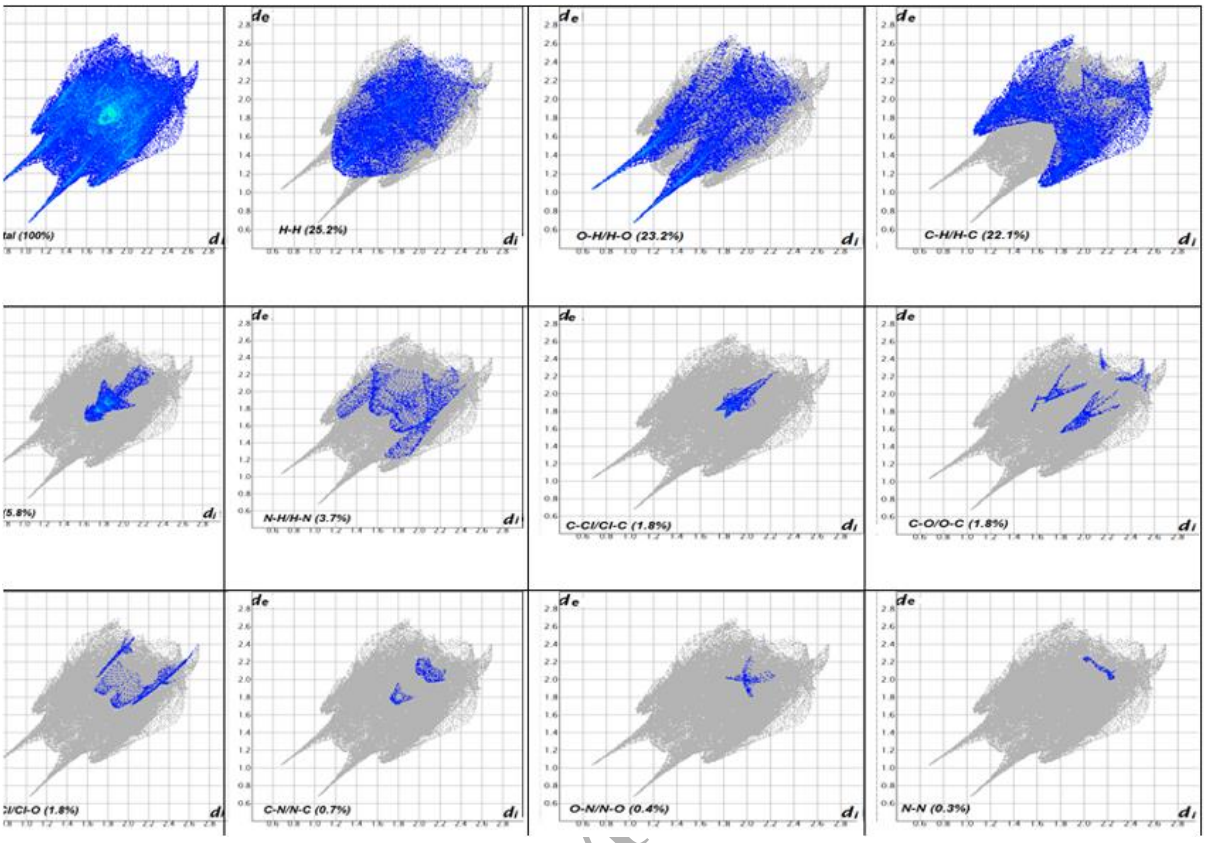

Fig. 6

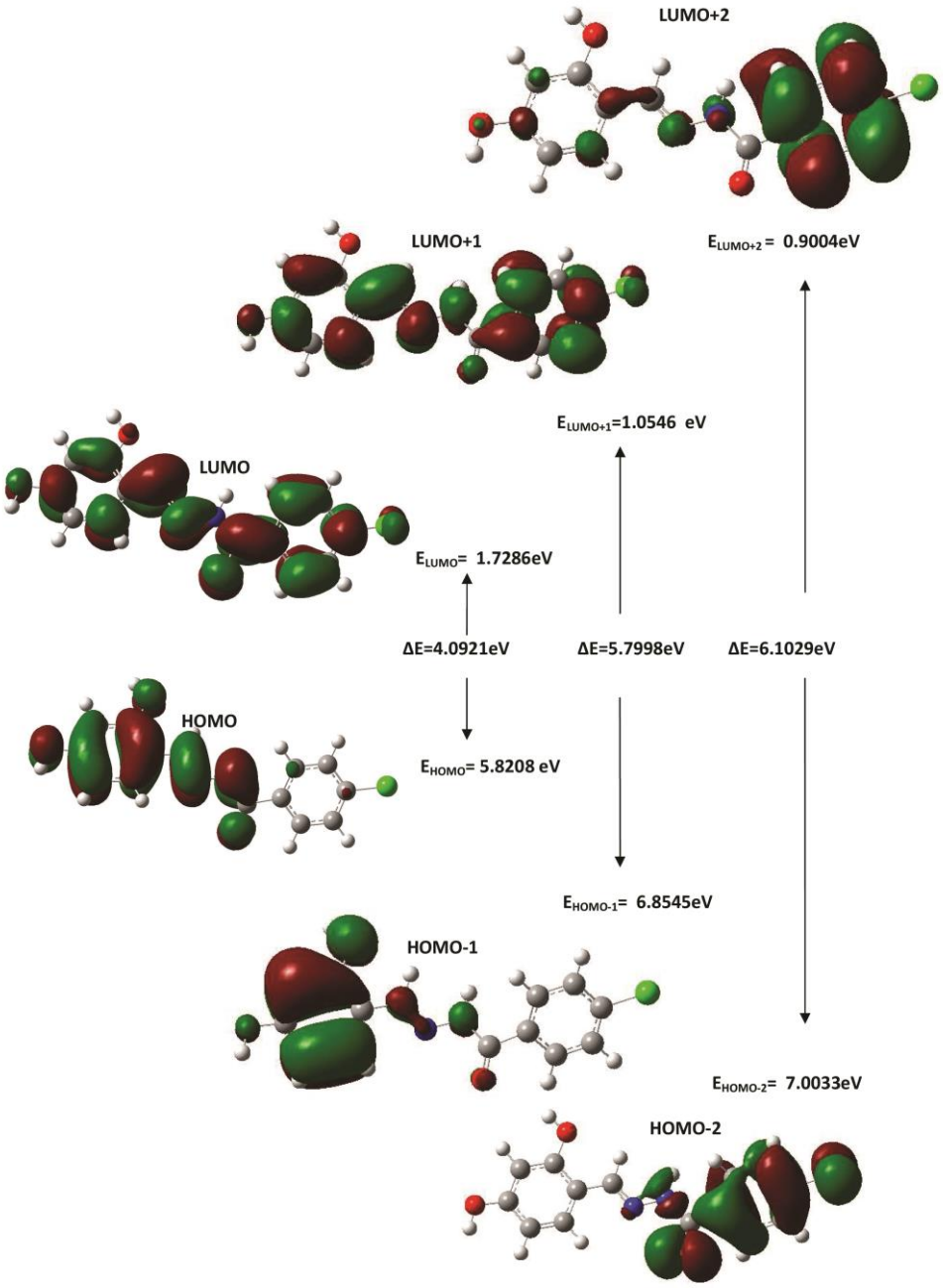
LUMO+2
LUMO+1
E_{LUMO+2} = 0.9004eV
E_{LUMO+1}=1.0546 eV
LUMO
E_{LUMO}= 1.7286eV
ΔE=4.0921eV
ΔE=5.7998eV
ΔE=6.1029eV
HOMO
E_{HOMO}= 5.8208 eV
E_{HOMO-1}= 6.8545eV
HOMO-1
E_{HOMO-2}= 7.0033eV
HOMO-2

Fig. 7

Graphical Abstract